JOURNAL OF COMPUTATIONAL PHYSICS 35, 77–89 (1980)

The Numerical Solution of the Unsteady Expansion of a Gas into a Near Vacuum

R. McLAUGHLIN

Department of Mathematics and Statistics, Sheffield City Polytechnic, Sheffield, United Kingdom

Received January 24, 1979; revised June 26, 1979

In this paper we consider the problem of the unsteady one-dimensional expansion of an initially uniform source gas into a non-uniform low density ambient atmosphere. We make a numerical study of the finite time solution of the contact front-primary shock regime using a particle path formulation of the characteristic equations of inviscid gas dynamics. The numerical method employed is a slightly modified version of that due to Hartree and we compare our results with the known asymptotic solutions.

1. INTRODUCTION

This paper presents a numerical study of the problem considered in [1, 2]. We consider a uniform source gas initially at rest within $r = 1$, in non-dimensional units, and surrounded by a stationary non-uniform atmosphere of lower density and sound speed. At time $t = 0$ the equalisation process is allowed to commence and the subsequent flow is studied from the viewpoint of inviscid gas dynamics.

A contact front separates the two gases and drives the primary shock ahead of it whilst, in general, a secondary shock forms behind the contact front. In the limiting case, the one discussed here, of the atmospheric density and sound speed being much lower initially than those of the source gas, the contact front moves, to a first approximation, with a speed equal to that of the gas–vacuum interface in the expansion *in vacuo*. It has been shown in [3] that this speed is independent of the one-dimensional geometry and it takes the value unity in our non-dimensional units of the next section. Because we have this simple boundary condition on the contact front, it is possible to consider the contact front-primary shock regime alone where the problem is now well-posed. For further details of the background to the problem, the reader is referred to [1].

The aim of this paper is to indicate how we numerically solve this problem for finite time and to compare sample numerical results with the asymptotic analysis of [1, 2].

The one-dimensional Eulerian equations are transformed using the particle path function so that both boundaries, the contact front and the shock, become known a priori. Two coordinate systems are used eventually and the solution of the equations is initiated by a "small time" perturbation scheme. The numerical method is a slightly

0021-9991/80/040077–13$02.00/0

modified version of the Specified Time Intervals or Backward Drawn Characteristics, devised by Hartree [4]. Hartree's method is described in Section 3 and it amounts to choosing a new mesh point and constructing the characteristic lines back to an earlier "time" where information on the dependent variables is known. This is in contrast to the more conventional method where one constructs characteristic lines from current mesh points forward to their point of intersection on a later "time" thereby producing, in general, a non-uniform mesh.

2. The Characteristic Equations and Boundary Conditions

All units used henceforth have been non-dimensionalised as in [1]. The nomenclature is such that u, p, ρ, a are respectively the gas velocity, pressure, density and sound speed with $a^2 = \gamma p/\rho$. The ratio of specific heats, γ, is assumed constant and σ, the geometry index, takes the values 0, 1, 2 respectively for plane, cylindrical and spherical symmetry. In addition r is the spatial coordinate, t is the time and $V_1(r)$ is the unknown shock velocity. The atmospheric density ahead of the shock is equal to r^{-k}, where k is some non-negative constant.

The starting point here is the familiar Eulerian equations in characteristic form, e.g., see [5],

$$\begin{aligned} &dp \pm \rho a\, du + \sigma \rho u a^2\, dt/r = 0 \qquad \text{on} \quad \frac{dr}{dt} = (u \pm a), \\ &d(p\rho^{-\gamma}) = 0 \qquad \text{on} \quad \frac{dr}{dt} = u \end{aligned} \tag{2.1}$$

with

$$u = 1 \qquad \text{on} \quad r = 1 + t \tag{2.2}$$

and the Rankine–Hugoniot shock relations

$$\begin{aligned} u &= 2V_1(r)/(\gamma + 1), \\ p &= 2V_1^2(r) r^{-k}/(\gamma + 1), \\ \rho &= (\gamma + 1) r^{-k}/(\gamma - 1) \end{aligned} \tag{2.3}$$

on $r = r_s(t)$ where $dr_s/dt = V_1(r_s)$, $r_s(0) = 1$.

We now introduce the particle path function ψ through

$$\frac{\partial \psi}{\partial r} = \rho r^{\sigma}, \qquad \frac{\partial \psi}{\partial t} = -\rho u r^{\sigma}$$

and define further variables by

$$\begin{aligned}
\phi &= (\sigma + 1 - k)\psi, && k < (\sigma + 1),\\
&= \psi, && k = (\sigma + 1),\\
&= \frac{(k - \sigma - 1)\psi}{1 - (k - \sigma - 1)\psi}, && k > (\sigma + 1),\\
y &= r^{|\sigma+1-k|} - 1, && k \neq (\sigma + 1),\\
&= \log_e r, && k = (\sigma + 1),\\
\theta &= \phi/y,
\end{aligned}$$

$$p = \tfrac{1}{2}(\gamma + 1)\, r^{-k}P, \qquad \rho = (\gamma + 1)r^{-k}R/(\gamma - 1), \qquad V_1(r) = \tfrac{1}{2}(\gamma + 1)\, V(r).$$

Using these new variables Eqs. (2.1) become

$$dP \pm \frac{2}{(\gamma - 1)}\, Ra\, du + \gamma P\left[\frac{\sigma u}{u \pm a} - k/\gamma\right]\frac{dy}{D(y)} = 0$$

on

$$\frac{d\phi}{dy} = \pm\frac{(\gamma + 1)Ra\, E(\phi, y)}{(\gamma - 1)(u \pm a)}, \qquad \frac{d\theta}{dy} = \frac{1}{y}\left[\frac{d\phi}{dy} - \theta\right], \tag{2.4}$$

$$d[PR^{-\gamma}f(y)] = 0 \qquad \text{on} \quad \frac{d\phi}{dy} = 0 \quad \text{or} \quad \frac{d\theta}{dy} = -\frac{\theta}{y}, \tag{2.5}$$

where

$$\begin{aligned}
D(y) &= |\,\sigma + 1 - k\,|\,(1 + y), && k \neq (\sigma + 1),\\
&= 1, && k = (\sigma + 1),\\
E(\phi, y) &= 1, && k \leqslant (\sigma + 1),\\
&= \left(\frac{1 + \phi}{1 + y}\right)^2 = \left(\frac{1 + \theta y}{1 + y}\right)^2, && k > (\sigma + 1),\\
f(y) &= (1 + y)^{k(\gamma-1)/|\sigma+1-k|}, && k \neq (\sigma + 1),\\
&= \exp[k(\gamma - 1)y], && k = (\sigma + 1),
\end{aligned}$$

and $a^2 = \frac{1}{2}\gamma(\gamma - 1)\, PR^{-1}$.

The boundary conditions (2.2), (2.3) now become

$$u = 1 \qquad \text{on} \quad \phi = \theta = 0,$$
$$u = V, \quad P = V^2, \quad R = 1 \qquad \text{on} \quad \phi = y \text{ or } \theta = 1.$$

Also the initial conditions, at $\phi = y = 0$ or $0 \leqslant \theta \leqslant 1$ with $y = 0$, are the locally plane solutions with $k = 0$, i.e., $u = P = R = V = 1$, and the region of integration is $0 \leqslant \phi \leqslant y$ or $0 \leqslant \theta \leqslant 1$, $0 \leqslant y < \infty$. It should be understood that (ϕ, y) and (θ, y) are alternative coordinate systems.

It is clear that the shock boundary is now known a priori and it is in fact a straight line in both coordinate systems. This fact reduces by one the number of approximations necessary in the subsequent discretisation.

3. Numerical Method and Stability Considerations

In this section we outline the numerical method as applied to the problem under discussion. For small y the characteristic curves in the (θ, y) coordinate system are almost parallel to the θ axis and initially a large value of $\Delta\theta$ would be needed for efficient integration. This value of $\Delta\theta$ would be inappropriate for larger values of y and we overcome the difficulty by commencing the numerical integration in the (ϕ, y) system. This system has, as we shall see, an inbuilt facility for systematically increasing the number of mesh points and thus effectively reducing the size of $\Delta\theta$. This facility is provided by the sloping shock boundary and we indicate later how it is used.

The advantage of Hartree's method is that it automatically produces solutions on a regular mesh, thereby dispensing with the need to store the coordinates of the mesh points in the computer memory. For a point neither too near nor on either boundary, Hartree's method is illustrated in Fig. 1 where τ represents either ϕ or θ.

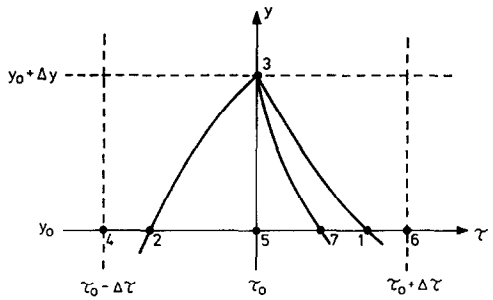

Fig. 1. Standard method.

Given values of the gas variables at points along the line $y = y_0$ we wish to find values at points on $y = y_0 + \Delta y$. Consider a typical mesh point, point 3 in Fig. 1, on $y = y_0 + \Delta y$. We construct the three characteristic curves from this point back to the line $y = y_0$ and apply the relevant compatibility condition along each characteristic curve. This cannot be done exactly but we carry it out approximately by applying a differencing scheme to the first four of equations (2.4); the first two of (2.5) are integrable. In this scheme we replace the differential of a quantity by the difference of its values at each end of the relevant characteristic and each coefficient by the mean of its values at each end of this characteristic. Second order interpolation is used to find values on $y = y_0$ in the interval $\phi_0 - \Delta\phi < \phi < \phi_0 + \Delta\phi$. Here $\phi_0 = \phi_5 = \phi_3$.

We illustrate the differencing approximation by considering the equations in the (ϕ, y) system. The first two of (2.4) are approximated by

$$(P_3 - P_2) + \frac{2}{(\gamma - 1)}\{Ra\}_{2,3}(u_3 - u_2) + \gamma\left\{\frac{P[\sigma u/(u + a) - k/\gamma]}{D(y)}\right\}_{2,3}(y_3 - y_2) = 0,$$

$$(P_3 - P_1) - \frac{2}{(\gamma - 1)}\{Ra\}_{1,3}(u_3 - u_1) + \gamma\left\{\frac{P[\sigma u/(u - a) - k/\gamma]}{D(y)}\right\}_{1,3}(y_3 - y_1) = 0.$$

where $\{X\}_{i,3} = \frac{1}{2}(X_i + X_3)$, $i = 1, 2$.

Rearranging, these become

$$\begin{aligned} P_3 + \frac{2}{(\gamma - 1)}\{Ra\}_{2,3}u_3 &= P_2 + \frac{2}{(\gamma - 1)}\{Ra\}_{2,3}u_2 \\ &\quad - \gamma\left\{\frac{P[\sigma u/(u + a) - k/\gamma]}{D(y)}\right\}_{2,3}\Delta y, \\ P_3 - \frac{2}{(\gamma - 1)}\{Ra\}_{1,3}u_3 &= P_1 - \frac{2}{(\gamma - 1)}\{Ra\}_{1,3}u_1 \\ &\quad - \gamma\left\{\frac{P[\sigma u/(u - a) - k/\gamma]}{D(y)}\right\}_{1,3}\Delta y. \end{aligned} \tag{3.1}$$

The second pair of (2.4), i.e., the equations for the characteristic curves in (ϕ, y) space, are approximated by

$$\begin{aligned} (\phi_3 - \phi_2) &= \left(\frac{\gamma + 1}{\gamma - 1}\right)\left\{\frac{Ra\,E(\phi, y)}{u + a}\right\}_{2,3}(y_3 - y_2), \\ (\phi_3 - \phi_1) &= -\left(\frac{\gamma + 1}{\gamma - 1}\right)\left\{\frac{Ra\,E(\phi, y)}{u - a}\right\}_{1,3}(y_3 - y_1). \end{aligned} \tag{3.2}$$

The first two of (2.5) are integrated to give $P_3R_3^{-\gamma}f(y_3) = P_7R_7^{-\gamma}f(y_7)$, i.e.,

$$\begin{aligned} R_3 &= R_7\left[\frac{P_3 f(y_3)}{P_7 f(y_7)}\right]^{1/\gamma}, \\ \phi_3 &= \phi_7 = \phi_5\,. \end{aligned} \tag{3.3}$$

With this last result, (3.3) becomes

$$R_3 = R_5(P_3/P_5)^{1/\gamma}[f(y_3)/f(y_7)]^{1/\gamma}. \tag{3.4}$$

In addition we still have

$$a = \tfrac{1}{2}\gamma(\gamma - 1)P/R. \tag{3.5}$$

Equations (3.1) and (3.2) comprise a set of four non-linear algebraic equations in the four unknowns P_3, u_3, ϕ_1, ϕ_2. Equations (3.4) and (3.5) are used as straight-

forward formulae and the six values P_1, P_2, u_1, u_2, R_1, R_2 are approximately by Lagrangian interpolation, e.g.,

$$P_i = \frac{(\phi_i - \phi_5)(\phi_i - \phi_6)}{(\phi_4 - \phi_5)(\phi_4 - \phi_6)} P_4 + \frac{(\phi_i - \phi_4)(\phi_i - \phi_6)}{(\phi_5 - \phi_4)(\phi_5 - \phi_6)} P_5 + \frac{(\phi_i - \phi_4)(\phi_i - \phi_5)}{(\phi_6 - \phi_4)(\phi_6 - \phi_5)} P_6, \qquad i = 1, 2. \tag{3.6}$$

Equations (3.1), (3.2) could be solved by a standard quasi-Newton (superlinear) iterative method but it was found that a linear iterative scheme was more efficient in terms of computer time. This linear iterative method is as follows: Equations (3.1) are regarded as 2 simultaneous "linear" algebraic equations in P_3 and u_3:

$$P_3 + A_1 u_3 = B_1,$$
$$P_3 - A_2 u_3 = B_2,$$

where

$$A_1 = \frac{2}{(\gamma - 1)} \{Ra\}_{2,3},$$

etc., the "solutions" of which are

$$P_3 = (A_1 B_2 + A_2 B_1)/(A_1 + A_2),$$
$$u_3 = (B_1 - B_2)/(A_1 + A_2). \tag{3.7}$$

In A_1, A_2, B_1, B_2 the current estimates for P_3, u_3, etc., are used, (3.7) then provides new estimates for P_3, u_3. Equations (3.2) are rewritten as

$$\phi_2 = \phi_3 - \left(\frac{\gamma + 1}{\gamma - 1}\right) \left\{\frac{Ra\, E(\phi, y)}{u + a}\right\}_{2,3} \Delta y,$$
$$\phi_1 = \phi_3 + \left(\frac{\gamma + 1}{\gamma - 1}\right) \left\{\frac{Ra\, E(\phi, y)}{u - a}\right\}_{1,3} \Delta y. \tag{3.8}$$

In the right-hand sides of (3.8) the current estimates of the unknowns are used and then the resulting values ϕ_2 and ϕ_1 are new estimates for ϕ_2 and ϕ_1.

Equations (3.7) and (3.8) together with the supporting "formulae" (3.4), (3.5), (3.6) comprise the linear iterative method. The sequence of calculation is: (3.4), a_3 from (3.5), (3.8), interpolation as in (3.6), and then (3.7). The values P_3, u_3, R_3 are of prime consideration, the values ϕ_1, ϕ_2, etc., are incidental. The iteration commences with the initial estimates: P_5 for P_1, P_2, P_3; u_5 for u_1, u_2, u_3; R_5 for R_1, R_2, R_3; ϕ_3 for ϕ_1, and ϕ_2. It ends when a sufficiently accurate solution to the algebraic equations is obtained.

The method is entirely similar in the (θ, y) coordinate system, only the resulting algebraic equations are slightly different.

When obtaining values at points on $\phi = \theta = 0$ only the negative characteristic and the streamline are used since we have the boundary condition $u = 1$. For points on $\phi = y$, $\theta = 1$ only the positive characteristic is used since we effectively have two boundary conditions in $R = 1$, $P = u^2 = V^2$. Clearly the number of algebraic equations is reduced in each case.

In the (ϕ, y) coordinate system the range of ϕ increases as we progress with the integration. This allows us to systematically increase the number of mesh points on lines of constant y. The size of Δy is restricted by stability conditions as we see later, and it is chosen so that $\Delta\phi/\Delta y$ is an integer, M, say. Suppose that we have the numerical solution at $K + 1$ equispaced points on $y = K\Delta\phi$, where K is some integer. On the next line, i.e., $y = K\Delta\phi + \Delta y$, the point which was on the shock for $y = K\Delta\phi$ is now a distance Δy from the shock and we introduce a new point on the shock at $\phi = y = K\Delta\phi + \Delta y$.

We systematically increase y by Δy, solving the algebraic equations each time, and the distance between the points on and adjacent to the shock increases until $y = (K + 1)\Delta\phi$, where we now have $K + 2$ equispaced points. The difficulty that may arise here is that, for the intermediate values of y, the negative characteristic curve from the point next to the shock may intersect the previous line of constant y at a value of ϕ which is greater than the value of y, i.e., outside the region of integration. If this were the case we would have to extrapolate to find values of the gas variables at the bottom of this characteristic, a state of affairs likely to induce instability, and we prevent this from happening by modifying Hartree's method.

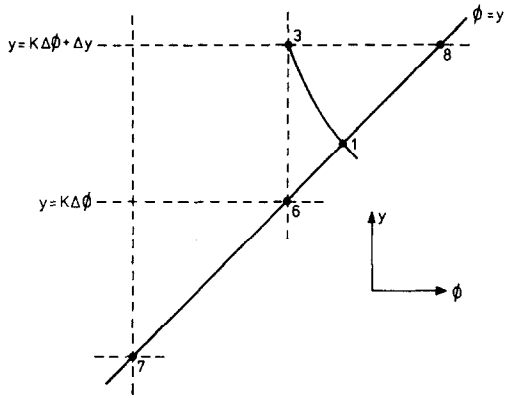

FIG. 2. Method modified for boundary.

Figure 2 illustrates the way in which we introduce the additional mesh point on the shock, point 8, and it also assists in our description of the modified method. We construct a shorter negative characteristic curve as shown and apply the negative compatibility condition between point 3 and point 1 which now lies on the shock boundary, $\phi = y$. Whether this negative characteristic reaches the shock first or not is determined by approximately solving a locally linearised version of the equation of

this curve. In addition values a point 1 are now found by Lagrangan interpolation using values at points 7, 6, and 8.

When integrating in the (θ, y) coordinate system no such difficulties arise and we use the standard method only.

The stability condition used is the Courant–Friedrichs–Lewy condition and this condition, if fulfilled, ensures that, away from sloping boundaries, extrapolation is avoided. For the problem under discussion this condition can be stated as

$$\Delta y \leqslant \alpha \Delta \tau$$

where τ represents either ϕ or θ and α is the average value of $| dy/d\tau |$ between the end points of a negative characteristic curve. To set an upper limit on Δy initially, near $y = 0$, we use the locally plane solution which implies

$$\beta = \frac{\Delta y}{\Delta \phi} \leqslant \frac{(\gamma - 1)}{(\gamma + 1)} \left\{ \left(\frac{2}{\gamma(\gamma - 1)} \right)^{1/2} - 1 \right\}.$$

In particular for $\gamma = 7/5$, $5/3$ this gives $\beta \leqslant 0.148$, 0.085, respectively, and we then use $\beta = 1/8$, $1/16$ to give Δy initially for a particular value of $\Delta \phi$. Subsequently a check is made on stability at each mesh point by considering the value ϕ_1 of ϕ at point 1 in Fig. 1. If $\phi_1 > \phi_6$ then Δy is too large and we return to $y = y_0$ with Δy replaced by $\Delta y/2$. This, however, was not found to be necessary in our two sample integrations.

Now that the details of the numerical method have been stated we indicate the overall algorithm. To initiate the solution we use the series solution for small y of the partial differential equations associated with (2.4), (2.5). These series are developed by letting

$$\begin{aligned} u &= 1 + y u_1(\theta) + y^2 u_2(\theta) + \cdots, \\ P &= 1 + y P_1(\theta) + y^2 P_2(\theta) + \cdots, \\ R &= 1 + y R_1(\theta) + y^2 R_2(\theta) + \cdots, \\ V &= 1 + y b_1 + y^2 b_2 + \cdots. \end{aligned}$$

The algebraic manipulations are quite straightforward and we illustrate the results up to $O(y)$ by considering $k < (\sigma + 1)$:

$$\begin{aligned} u_1(\theta) &= b_1 \theta, \\ R_1(\theta) &= a_1(1 - \theta), \\ P_1(\theta) &= 2b_1\theta + \left\{ \gamma a_1 - \frac{k(\gamma - 1)}{(\sigma + 1 - k)} \right\} (1 - \theta), \end{aligned}$$

with

$$a_1 = \frac{(\gamma - 1)\{k(\gamma + 1) - 2\sigma\}}{2(2\gamma - 1)(\sigma + 1 - k)}$$

and

$$b_1 = \frac{-(\gamma - 1)\{k(\gamma^2 - 4\gamma + 1) + 2\gamma\sigma\}}{2(\gamma + 1)(2\gamma - 1)(\sigma + 1 - k)}.$$

The second order terms u_2, P_2, R_2 can be obtained and they are quadratic functions of θ but the algebra becomes extremely involved for higher orders. Similar results are obtained for $k \geqslant (\sigma + 1)$.

We use these series solutions up to second order to provide values of u, P, R at three equispaced points on $y = 2\Delta\phi$, i.e., at $\phi = 0$, $\Delta\phi$, $2\Delta\phi$, and V for $y = 2\Delta\phi$ and then commence the numerical integration. The (ϕ, y) coordinate system is used until $y = 1$ when we change to the (θ, y) system with $\Delta\theta = \Delta\phi$. Since $d\theta$ is approximately proportional to $\Delta y/y$ we double Δy at $y = 2$, 4, 8, etc. until $\Delta y = \Delta\theta$. This accelerates the integration but ensures that stability conditions are not violated and that the local truncation error is held at $O(\Delta\theta^3)$.

4. Numerical Results and Comparison with the Asymptotic Analysis

The initial motivation for producing numerical results for our problem was to provide a check for the asymptotic theory developed in [1, 2]. For this comparison it was necessary to produce the numerical solutions accurately and so we choose $\Delta\phi = 0.01$. For less critical uses of the numerical results a larger value of $\Delta\phi$ could be used.

Even though the integrations were carried out in the particle path coordinate systems we display the results in a more physical form so that they may, if necessary, be compared with experimental results. Briefly we plot the various results as functions of η, where

$$\eta = \frac{r - 1 - t}{r_s - 1 - t}$$

and r_s is the physical position (or radius) of the shock at time t. The boundaries $\theta = 0$, 1 become $\eta = 0$, 1, respectively, and, as $t \to \infty$, we have

$$\eta \to \frac{\lambda - 1}{\lambda_s - 1} \qquad \text{for} \quad k < k_c,$$

$$\eta \to \frac{\lambda}{\lambda_s} \qquad \text{for} \quad k > k_c.$$

where $\lambda = rt^{-\delta}$ is the similarity variable and k_c is a critical value of k found in [1, 2].

In what follows the symbol ∞ is used to label information derived from the asymptotic analysis and the suffix s indicates values at the shock.

Two cases were chosen for numerical investigation and these are now discussed.

Case I. In this case we have $\sigma = 2$, $\gamma = 7/5$, $k = 1 < k_c$. The variables u, $P(r/r_s)^{-k}$, $R(r/r_s)^{-k}$ are plotted in Figs. 3–5, the factor r/r_s becoming λ/λ_s as $t \to \infty$. Values of r_s and V_1 are given in Table I. It can be seen from these results that the flow quickly settles down to its asymptotic state and it is worth noting that, in the (θ, y) coordinate system at about $r = 8$, the difference between the asymptotic and finite time solutions is less than 1 %.

TABLE I

t	r_s	V_1
0	1	1.2
0.2	1.236	1.1655
0.6	1.694	1.1253
1.0	2.140	1.1079
1.5	2.691	1.0965
2.0	3.238	1.0910
6.0	7.580	1.0838
∞	∞	1.0832

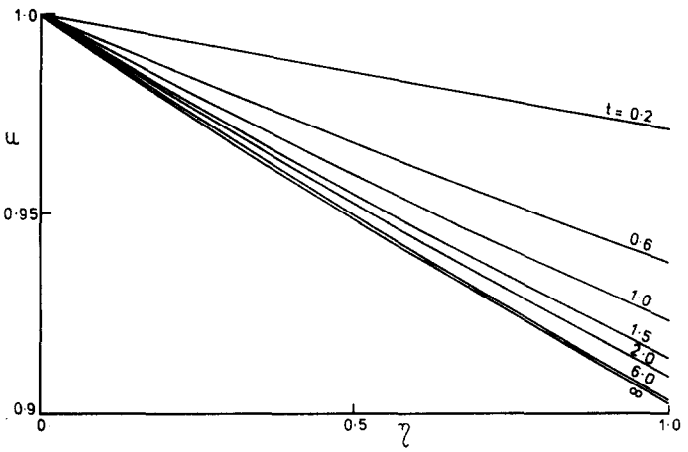

FIG. 3. u vs η for Case I.

Caes II. Now we have $\sigma = 2$, $\gamma = 5/3$, $k = 3.5 > k_c$. Since the shock velocity can be expected to increase without bound as t increases, we display the functions u/u_s, $P/P_s(r/r_s)^{-k}$, $R(r/r_s)^{-k}$ in Figs. 6–8, the factor r/r_s again becoming λ/λ_s as $t \to \infty$. Values of r_s and V_1 for this case are given in Table II. It can be seen from these graphs that the flow takes quite a long time to settle down to its asymptotic state; the reasons for this are given in [1].

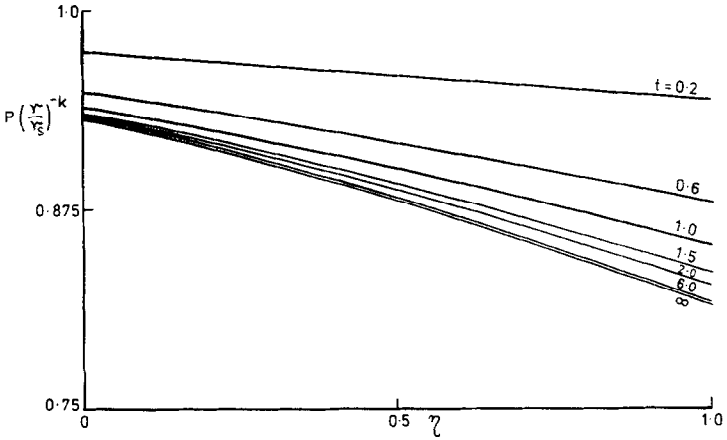

FIG. 4. $P(r/r_s)^{-k}$ vs η for Case I.

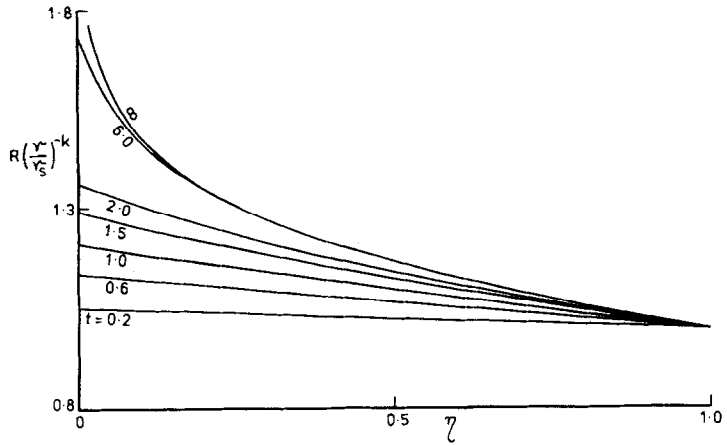

FIG. 5. $R(r/r_s)^{-k}$ vs η for Case I.

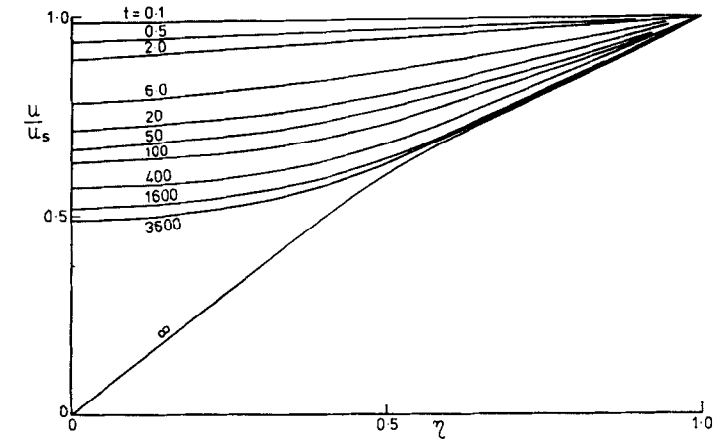

FIG. 6. u/u_s vs η for Case II.

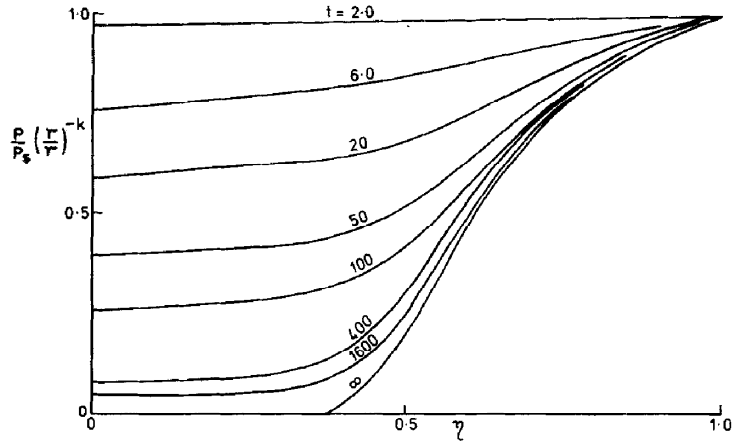

FIG. 7. $P/P_s(r/r_s)^{-k}$ vs η for Case II.

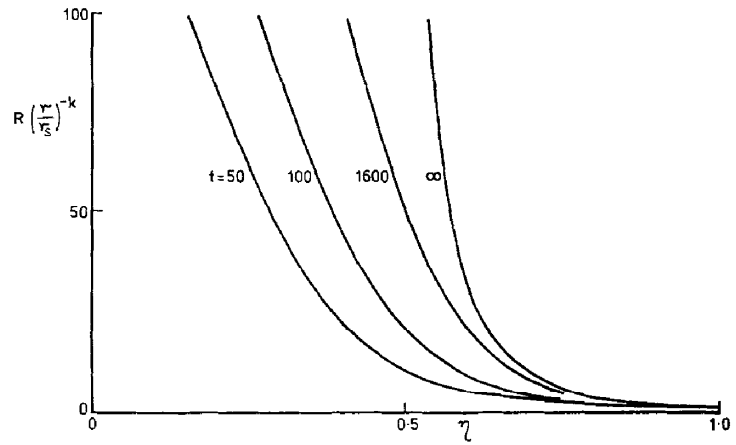

FIG. 8. $R(r/r_s)^{-k}$ vs η for Case II.

To compare these solutions further with the asymptotic analysis we fit functions of the form αr^{β} to P on $\theta = 0$ and V_1 at large r by regressional analysis to obtain

$$P \simeq 184 r^{-1.51} \quad \text{on} \quad \theta = 0,$$

$$V_1 \simeq 1.51 r^{0.065}$$

The asymptotic analysis predicts respectively $k - \gamma(\sigma + 1)$ and $\epsilon = 1/(\delta - 1)$, a function of k, γ and σ, for these two exponents, or -1.5 and 0.0647 in this case, a very good agreement. It can be seen from Figs. 6–8 that, for small η, the finite time solutions do not compare favourably with the asymptotic solutions. The reason for this is that the asymptotic expansions are no longer valid and then, as shown in [1, 2], different series expansions are sought.

TABLE II

t	r_s	V_1
0	1	1.333
0.1	1.134	1.357
0.5	1.693	1.430
1.0	2.425	1.488
2.0	4.036	1.552
6.0	10.56	1.71
20	35.93	1.88
50	94.45	2.02
100	198.3	2.12
400	867.4	2.34
900	2046	2.47
1600	3749	2.57
2500	6000	2.65
3600	9116	2.72

In conclusion we have indicated how to numerically solve the problem and we have shown that, for the two cases chosen, the finite time solutions do in fact approach the forms predicted by the asymptotic analysis of [1, 2].

ACKNOWLEDGMENTS

The author would like to thank Dr. R. E. Grundy for his helpful comments and also the Science Research Council for a supporting grant.

REFERENCES

1. R. MCLAUGHLIN, Ph.D. thesis, University of St. Andrews, 1975.
2. R. E. GRUNDY AND R. MCLAUGHLIN, *J. Fluid Mech.* **81** (1977), 775.
3. H. P. GREENSPAN AND D. S. BUTLER, *J. Fluid Mech.* **13** (1962), 101.
4. D. R. HARTREE, "Numerical Analysis," 2nd ed., Oxford Univ. Press, London/New York, 1958.
5. R. COURANT AND K. O. FRIEDRICHS, "Supersonic Flow and Shock Waves," Interscience, New York, 1948.